atmosphere

MDPI

Article

Large Amounts of Water Vapor Were Injected into the Stratosphere by the Hunga Tonga–Hunga Ha'apai Volcano Eruption

Jingyuan Xu [1,2], Dan Li [1,*], Zhixuan Bai [1], Mengchu Tao [1,3] and Jianchun Bian [1,2,4]

[1] Key Laboratory of Middle Atmosphere and Global Environment Observation, Institute of Atmospheric Physics, Chinese Academy of Sciences, Beijing 100029, China; xujingyuan@mail.iap.ac.cn (J.X.); baizhixuan@mail.iap.ac.cn (Z.B.); mengchutao@mail.iap.ac.cn (M.T.); bjc@mail.iap.ac.cn (J.B.)
[2] College of Earth and Planetary Sciences, University of Chinese Academy of Sciences, Beijing 100049, China
[3] Carbon Neutrality Research Center, Institute of Atmospheric Physics, Chinese Academy of Sciences, Beijing 100029, China
[4] College of Atmospheric Sciences, Lanzhou University, Lanzhou 730000, China
* Correspondence: lidan@mail.iap.ac.cn

Abstract: The Hunga Tonga–Hunga Ha'apai (Tonga) injected only small amount of SO_2 into the stratosphere, while our analyses of the Microwave Limb Sounder (MLS) measurements show that a massive amount of water vapor was directly injected into the stratosphere by the Tonga eruption, which is probably due to its submarine volcanic activity. The Tonga eruption injected a total amount of 139 ± 8 Tg of water vapor into the stratosphere and resulted in an increase of 8.9 ± 0.5% in the global stratospheric water vapor. Analyses also show that the uppermost altitude impacted by Tonga reached the 1 hPa level (~47.6 km). Additionally, the maximum hydration region for increased water vapor is at 38–17 hPa (~22.2–27 km), where the water vapor mixing ratio increased by 6–8 ppmv during the three months after the Tonga eruption. The enhanced stratospheric water vapor has great potential to influence the global radiation budget as well as ozone loss.

Keywords: stratospheric water vapor; Tonga; volcanic injected hydration

Citation: Xu, J.; Li, D.; Bai, Z.; Tao, M.; Bian, J. Large Amounts of Water Vapor Were Injected into the Stratosphere by the Hunga Tonga–Hunga Ha'apai Volcano Eruption. *Atmosphere* **2022**, *13*, 912. https://doi.org/10.3390/atmos13060912

Academic Editor: Yoshihiro Tomikawa

Received: 23 May 2022
Accepted: 2 June 2022
Published: 4 June 2022

1. Introduction

Stratospheric water vapor plays an important role in chemistry and global climate change. The increased water vapor in the stratosphere had the potential to enhance the rate of surface warming during the 1990s [1]. The increased water vapor in the mid-latitude stratosphere will contribute to ozone loss [2,3] and impede polar stratospheric ozone recovery [4].

Tropospheric air primarily enters the stratosphere across the tropical tropopause under the mean upward tropical Brewer–Dobson circulation. Vapor in excess of ice saturation is removed by the growth and sediment of ice crystals, called freeze drying [5]. When air parcels pass through the low temperature region at the convective outflow of tropical cyclones, the dehydration process occurs [6]. In addition to the dominant role of cold point temperature on stratospheric water vapor, other mechanisms such as methane oxidation, convective hydration, the quasi-biennial oscillation, and volcanic aerosol burden also contribute to the variation in stratospheric water vapor [7–10].

Previous studies have shown that volcanic eruptions can directly inject water vapor into the stratosphere [11–16], but this impact only lasts for a few days, and has a minor disturbance on the background level of the stratospheric water vapor. In situ frost point hygrometer measurements from an aircraft campaign determined ~40 ppmv water vapor mixing ratio in the plume of Mount St. Helens [12]. According to the estimation by Pitari et al. [16], 37.5 Tg of water vapor was injected into the stratosphere due to the

Pinatubo eruption. Lower stratospheric water vapor mixing ratios exceeding 10 ppmv were observed by the Microwave Limb Sounder (MLS) a few days after the 2015 Calbuco eruption [13] and 2 Tg of mass of stratospheric water vapor was inferred. We notice that these volcanic events originated from continents, while submerged volcano eruptions might be capable of injecting greater amounts of water vapor into the stratosphere.

The submarine Hunga Tonga–Hunga Ha'apai volcano (20.54° S, 175.38° W, referred to as Tonga) erupted violently on 15 January 2022, which is located near the South Pacific islands in the Kingdom of Tonga [17–19]. Tonga eruptive activity produced an unsteady volcanic plume that transiently reached 58 km into the mesosphere, corresponding to a Volcanic Explosivity Index (VEI) of 5–6 for this event. During an eruption duration of ~12 h, the eruptive volume and mass are estimated at 1.9 km^3 and ~2900 Tg, respectively [20].

Using a combination of remote sensing and in situ measurements, the MLS and balloon-borne Cryogenic frost point hygrometer (CFH) observations, we investigate and evaluate the influence of the Tonga eruption on stratospheric water vapor from the following two aspects:

1. To quantify the magnitude of the stratospheric water vapor increase caused by the Tonga eruption;
2. To evaluate the spatial and temporal extent of water vapor injected directly into the stratosphere as a result of the Tonga eruption.

2. Data and Methods

2.1. Data

Our analyses are based on remote sensing observations of water vapor from the MLS/Aura. We used the MLS daily water vapor profiles version 4.2 with a vertical resolution of 1.3–3.6 km from 316–0.22 hPa. More important for this study, MLS data has 25 vertical levels within 100–1 hPa. At 100, 22, and 1 hPa, the precision for a single profile of water vapor is 15%, 5%, and 6%, respectively [21]. The data screening criteria of quality (>0.7) and convergence (<2) specified by Livesey et al. [21] failed to distinguish anomalously high water vapor caused by the Tonga volcano. Therefore, appropriate data screening criteria were applied to avoid misjudgment. Data with status (an even number), precision (>0), and mixing ratio (>0.101 ppmv) at any pressure greater than or equal to 1 hPa (i.e., altitudes below that pressure level) were used.

In situ water vapor measurements with balloon-borne CFH are widely accepted as a standard for tropospheric and stratospheric water vapor measurements [22]. In our study, the balloon was launched at Lijiang (100.22° E, 26.85° N), Yunnan province on 9 April 2022 in the frame of the Sounding Water vapor, Ozone, and Particle (SWOP) campaign [23–25]. A CFH was attached to detect water vapor, with a small uncertainty (<0.2 K) in frost-point temperature and a corresponding uncertainty (2–3%) in water vapor volume mixing ratio [26].

In order to determine the propagation of exceptionally high water vapor in the stratosphere after the Tonga eruption, the European Centre for Medium-Range Weather Forecasts reanalysis (ERA5) data [27] was used to display the stratospheric wind field. The ERA5 data was recorded on a 0.25° × 0.25° horizontal grid and on 137 hybrid levels from surface to 0.01 hPa.

2.2. Methodology

The total mass of stratospheric water vapor was approximately calculated by the sum of water vapor mass within 100–1 hPa (~16.6–47.6 km), which could be divided into 24 vertical layers according to MLS pressure levels. We derived the mass of water vapor at each layer by accumulating the water vapor mass within each latitudinal band that is divided into 45 bins:

$$M = \sum_{n=1}^{24} m_n \quad (1)$$

With

$$m_n = \sum_{i=1}^{45} \frac{(P_n - P_{n+1}) \cdot S_i}{g} \cdot \epsilon \cdot r_{in} \quad (2)$$

Here, P_n and P_{n+1} are the pressure boundaries of the n-th layer, S_i means the area of the i-th latitudinal band, and r_{in} denotes the average mixing ratio of water vapor in the n-th layer and the i-th latitudinal band, $g = 9.81$ N kg^{-1} and $\epsilon = 0.622$. We note that there are no MLS water vapor measurements in the latitude range of 82–90°, where the water vapor mixing ratio of 78–82° is used instead.

3. Results

The motivation for this work comes from the enhanced water vapor at ~25–26 km derived from in situ measurements in Lijiang on 9 April 2022. For determination of the correlation between the observed enhancement and the Tonga eruption, we examined the daily MLS water vapor profiles from the time of the outbreak for Tonga. The results are illustrated in Figure 1, together with the corresponding ERA5 wind field. The tropical easterly jet stream at 30 hPa covered the region of 20° S–5° N, where Tonga (20.57° S, 175.38° W) was located at the southern edge of the jet. Isolated maxima of water vapor (>200 ppmv) were observed downwind of Tonga, showing excellent agreement between the water vapor outliers near the Tonga volcano and the horizontal wind field around 30 hPa level during 16–26 January 2022. These moist air parcels were transported one circle in the stratosphere along with the tropical easterly jet stream over a period of ~12 days.

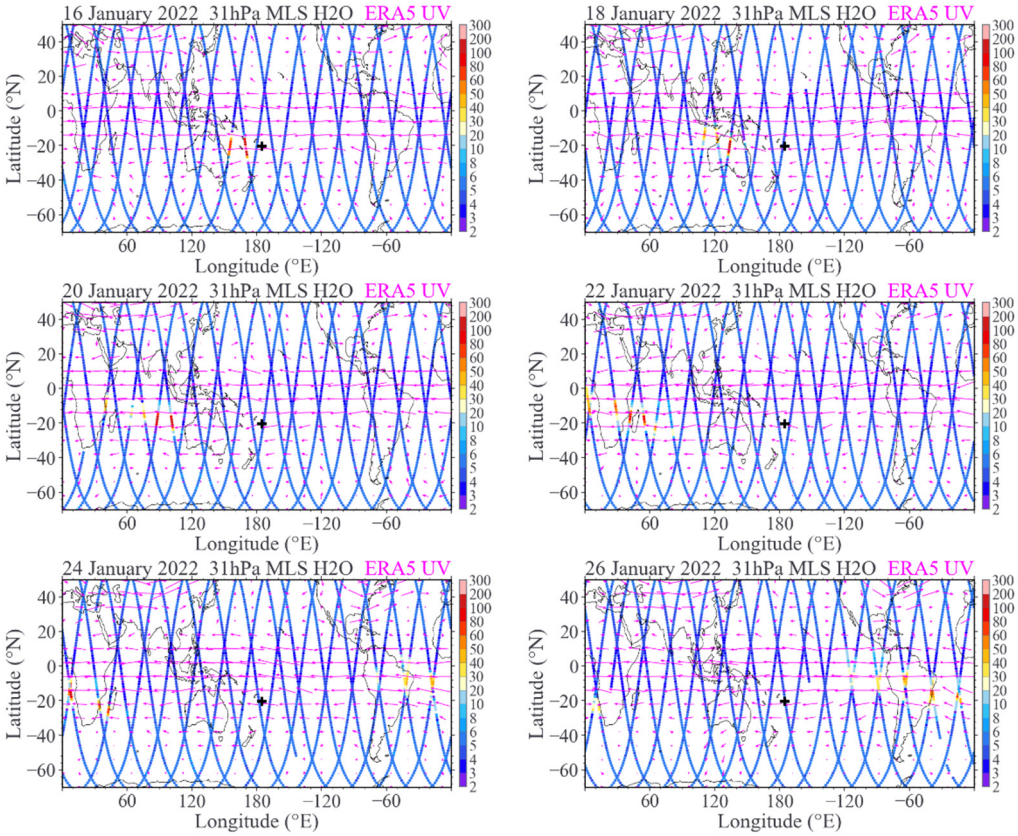

Figure 1. Water vapor (dots) mixing ratio (VMR, ppmv) at 31 hPa derived from MLS/Aura and wind field (magenta vectors) from the ERA5 reanalysis at 30 hPa at 00:00 UTC during 16–26 January 2022. The plus sign marks the location of Tonga near 20° S, 175° W.

The unprecedented enhanced water vapor (>200 ppmv) measured in Figure 1 far exceeds the stratospheric mean value (~4–5 ppmv) at the same pressure level. This provides convincing evidence that large amounts of water vapor were directly injected into the stratosphere due to the underwater volcano. Although the ash and SO_2 from El Chichon (1982) and Mount Pinatubo (1991) volcanoes had significant effects on the earth's climate, both of them originated from the continent. To further describe the effect of the Tonga eruption on stratospheric water vapor, we examined hundreds of water vapor profiles over 100–1 hPa, covering the period from 5 January to 25 April 2022. MLS water vapor anomalies were calculated to highlight the variation in water vapor after volcanic eruptions, by subtracting water vapor averaged 0–10 days prior to the eruption of Tonga, as shown in Figure 2a.

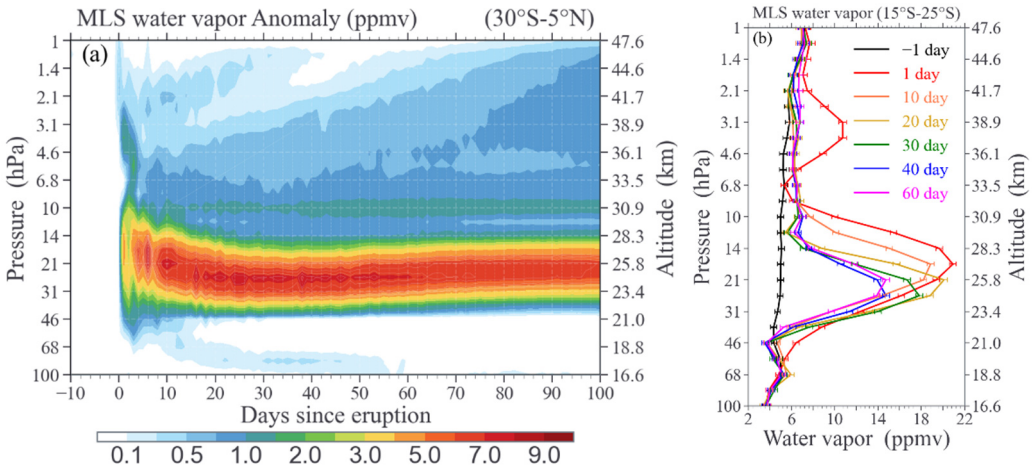

Figure 2. (**a**) MLS/Aura time series of mean (30° S–5° N) stratospheric water vapor anomalies (ppmv) from 100 to 1 hPa after the Tonga eruption (15 January 2022), during January–April 2022. The anomalies are calculated by subtracting water vapor averaged 0–10 days prior to the eruption of Tonga from daily water vapor data. (**b**) Stratospheric water vapor profiles on various days following the Tonga eruption. A narrower latitude range (15°–25° S, closer to Tonga) was chosen to highlight the effect of the eruption.

Figure 2a shows the significant effect of the Tonga volcano on stratospheric water vapor, which can reach 1 hPa level (~47.6 km) and persist for more than three months. Such a high plume height and long period of hydration are substantially stronger than previous volcanic records [11–13], indicating the unprecedented impact on stratospheric water vapor of the Tonga eruption. There is a maximum area for enhanced water vapor at pressure levels of 38–17 hPa (~22.2–27 km, Figure 2a,b), where water vapor mixing ratio is increased by 6–8 ppmv. Given the plume dispersion, the stratospheric water vapor profiles approach the background value as time goes on (Figure 2b) but retain a maximum value (>12 ppmv) over ~30–20 hPa. In addition, we note that the variation in water vapor in the lower stratosphere over 100–46 hPa (~16.6–21 km, Figure 2a,b) is almost invisible, which differs from the observed enhancement of lower stratospheric water vapor by Sioris et al. [13]. These results confirm the strong upwelling plume and a great amount of direct injection of water vapor into the stratosphere caused by the Tonga eruption.

In the maximum area for water vapor at pressure levels of 38–17 hPa (~22.2–27 km), we subtracted averaged water vapor 0–10 days prior to the eruption of Tonga to derive the horizontal propagation of stratospheric water vapor anomalies, as shown in Figure 3a. The anomalous water vapor rapidly diffused along with the easterly jet from the injection site (black plus sign) during the first 12 days and was concentrated in the 30° S–5° N, with a subsequent slow spread to mid-latitudes. Another irrefutable line of evidence of stratospheric water vapor enhancement and dispersion is the in situ observation launched in the North Hemisphere (26.8° N, 100.2° E) 84 days after Tonga erupted. Figure 3b shows the balloon-borne CFH measurements on 9 April 2022 in Lijiang, Yunnan (black triangle in

Figure 3a), which captures the enhanced water vapor (5–9 ppmv, relative to a background value of about 4–5 ppmv) over ~30–20 hPa levels, approximately consistent with MLS water vapor (5–7 ppmv). The MLS water vapor was derived from a profile (26.7° N, 108.6° E) at the same latitude as Lijiang, ~830 km apart from the CFH launch site with a 4-h lag. The MLS water vapor is a slightly drier than the CFH measurements between 22 and 26 hPa over the Tibetan Plateau, which was confirmed by former observations [28].

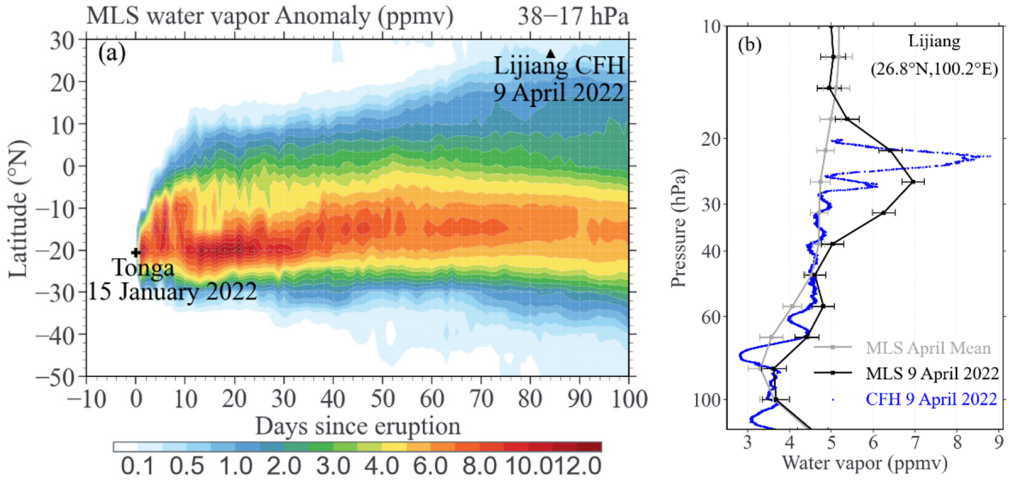

Figure 3. (**a**) Zonal mean water vapor anomalies (ppmv) as a function of latitude and time over 38–17 hPa levels. The locations of Tonga volcano and Lijiang are marked with a black plus sign and a triangle, respectively. (**b**) Vertical profiles of water vapor at Lijiang on 9 April 2022, derived from in situ observation (blue), and MLS remote sensing observation (black). The gray line shows the mean April water vapor with standard deviations derived from MLS during 2005–2020.

To quantify the influence of the Tonga eruption on global stratospheric water vapor, the calculations below are based on the estimation method mentioned in Section 2.2. The difference in the total mass of stratospheric water vapor after and before the Tonga eruption provides an estimate of the injected water vapor.

Time series for the daily variation in the total mass of stratospheric water vapor before and after the Tonga eruption are illustrated in Figure 4. The results demonstrate an increase of about 139 ± 8 Tg (8.9 ± 0.5%) for stratospheric water vapor. The total mass of stratospheric water vapor has increased from 1557 ± 1 to 1696 ± 8 Tg (1 Tg = 10^{12} g). Glaze et al. [11] suggested that the entire stratosphere contains 1400 Tg of water vapor, and their simulations showed that violent volcanic eruptions (such as Pinatubo-sized eruption) possess the capacity to inject more than 96 Tg (or 7%) water vapor into the stratosphere. This provides strong support for our estimation of 139 ± 8 Tg water vapor injected into the stratosphere by Tonga.

We calculated the total mass of stratospheric water vapor per unit area based on the MLS and in situ CFH measurements (Figure 3b) on 9 April 2022, respectively, to assess the uncertainty of MLS remote sensing measurements of water vapor. Results show that the total mass of stratospheric water vapor per unit area calculated by MLS is 2.65 g m^{-2}, which reasonably agrees with the quantification by CFH (2.52 g m^{-2}). In addition, a similar calculation was applied to the mean MLS water vapor in April during 2005–2020, which comes out to be 2.33 g m^{-2}. Referring to this mean water vapor mass, the relative increase is 13.7% according to MLS and 8.2% according to the CFH.

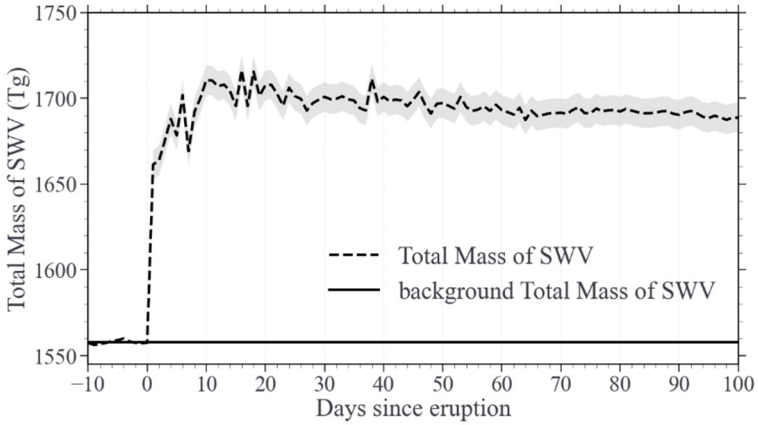

Figure 4. Time series of the total mass of stratospheric water vapor (SWV, 1 Tg = 10^{12} g) before and after the Tonga eruption (15 January 2022). The shaded region shows the standard deviation of the total mass of stratospheric water vapor during 100 days after the eruption. The solid line is shown for the total mass of SWV averaged 0–10 days prior to the eruption of Tonga, which is set as a background value.

4. Summary and Discussion

Volcanic eruptions can directly inject water vapor into the stratosphere based on theoretical research and measurements [12,13,16]. The main objectives of this study were to evaluate the spatial and temporal extent of the Tonga volcanic eruption on stratospheric water vapor and to quantify the magnitude of injected volcanic water vapor.

Based on MLS measurements, an estimation of the stratospheric water vapor increase is 139 ± 8 Tg (8.9 ± 0.5%), caused by the Tonga eruption (Figure 4). The volcanic plume transiently reached 58 km in the mesosphere [20], with the corresponding observed water vapor injection transiently reaching 1 hPa level (~47.6 km) in our results (Figure 2a). The increased water vapor was transported full circuit along with the easterly jet during the first 12 days and rapidly diffused to be concentrated in the 30° S–5° N (Figures 1 and 3a). Then, in the subsequent period of three months, direct injected hydration of the stratosphere due to the Tonga eruption mainly occurred over ~38–17 hPa (~22.2–27 km) levels, where water vapor mixing ratio increased by 6–8 ppmv (Figure 2a). Meanwhile, the anomalously high water vapor continuously spread to the mid-latitude and was captured by the in situ measurements at Lijiang (26.8° N, 100.2° E) 12 weeks after the Tonga eruption (Figure 3b).

Previous research provided various estimates of the total erupted mass of stratospheric water vapor. Given the volume of the plume as 2 × 10^6 km^3 [29] and an average mixing ratio in the plume of 20 ppmv from an aircraft campaign, Murcray et al. [12] calculated that a total mass of 3.2 Tg of water vapor was injected by the Mount St. Helens eruption (on 18 May 1980). Estimates of the total erupted mass from Mount St. Helens was 870 Tg [30] and a study by Rutherford et al. [31] found 4.6 ± 1% volatiles in the erupted melt, which are considered to be predominantly water vapor. Thus, a mass of ~40 Tg of water vapor is inferred from the Mount St. Helens eruption.

The mass of stratospheric water vapor injected by the Calbuco eruption (on 22 April 2015) was determined using MLS satellite observations [13]. Removing negative concentration anomalies relative to the background, the Calbuco water vapor mass enhancement of 1.5 Tg is estimated in the stratosphere, whose largest sources of uncertainty come from the longitudinal extent of the water vapor enhancement and the uniformity of the water vapor within the plume.

It is important to reiterate that there are similar uncertainties in our estimates of stratospheric water vapor injected by Tonga. According to the method mentioned in Section 2.2, substituting with water vapor of 78°–82° due to the lack of water vapor measurement within the pole (82°–90°) regions is a source of value for estimating the total mass of stratospheric water vapor. However, simulations from three CLaMS cases in Tao et al. [9] show little difference in water vapor between the two latitudinal bands.

Consequently, the above approximate substitution would have little error due to the small area of poles. Moreover, the method for estimating the total mass of stratospheric water vapor is highly dependent on the precision and accuracy of the MLS data. In comparison with the CFH measurements, the MLS measurements have a 5.3% wet bias in estimating the total mass of stratospheric water vapor.

As a result of filtering anomalously high stratospheric water vapor, MLS data quality limitation (>0.7) and convergence limitation (<2.0) were not used, especially during the first 2 weeks after eruption. However, additional adverse influences on stratospheric water vapor cannot be found in Figure 1 under such loose data screening. We also conducted sensitivity control experiments that using strict quality and convergence limitations had little effect on our results at least 2 weeks after the eruption (not shown).

Most of the "shallow branch" of Brewer–Dobson circulation is below 70 hPa [32], while the water vapor injected by the Tonga volcano is concentrated at 38–17 hPa. Therefore, the increased stratospheric water vapor would be transported to higher latitude mainly by the "deep branch" of Brewer–Dobson circulation (see Figure 2a). Such a single-cell poleward circulation transports from the tropics into the winter hemisphere [33], which explains why we captured the increase in water vapor at Lijiang in the Northern Hemisphere. According to our results, the increased stratospheric water vapor has not yet spread to the poles currently. However, the "deep branch" circulation and the meridional mixing driven by planetary and synoptic-scale Rossby waves breaking would continuously transport water vapor to higher latitudes and may have a significant impact on ozone chemistry [34,35].

Our overall results demonstrate that a large amount of water vapor is injected into the stratosphere by the Tonga volcanic eruption, which is one to two orders of magnitude greater than calculations of the Mount St. Helens [12] and Calbuco [13] eruptions. Additionally, unlike the short-lasting increase in stratospheric water vapor (e.g., ~9 days for 1980 Mount St. Helens; ~1 week for 2015 Calbuco), the water vapor injected by the submarine Tonga volcanic eruption has been present for several months in the stratosphere. Though the Tonga eruption had insignificant impacts on the global climate according to the weak intensity of SO_2 injection [36,37], a large amount of water vapor in the stratosphere posts extreme challenges for stratospheric chemistry and radiation budget. Future studies are required to assess the potential effects of this stratospheric injected hydration event.

Author Contributions: Conceptualization, J.B. and D.L.; methodology, J.B.; data campaign, Z.B.; visualization, J.X.; writing, J.X., D.L. and M.T. All authors gave comments and proofread the manuscript. All authors have read and agreed to the published version of the manuscript.

Funding: This work was partially supported by the second Tibetan Plateau Scientific Expedition and Research Program (STEP, 2019QZKK0604), the National Natural Science Foundation of China (Grant Nos. 91837311, 41975050 and 41905041), and a joint NSFC–DFG research project (NSFC grant no. 42061134012).

Institutional Review Board Statement: Not applicable.

Informed Consent Statement: Not applicable.

Data Availability Statement: The balloon data in Lijiang are available upon request to Jianchun Bian (bjc@mail.iap.ac.cn). ERA5 meteorological reanalysis data can be downloaded for free from the web page http://apps.ecmwf.int/datasets/, accessed on 21 April 2022. The MLS and water vapor data were downloaded from https://acdisc.gesdisc.eosdis.nasa.gov/data/, accessed on 20 April 2022.

Acknowledgments: We would like to thank Holger Vömel for post-processing the CFH data.

Conflicts of Interest: The authors declare no conflict of interest.

References

1. Solomon, S.; Rosenlof, K.H.; Portmann, R.W.; Daniel, J.S.; Davis, S.M.; Sanford, T.J.; Plattner, G.K. Contributions of Stratospheric Water Vapor to Decadal Changes in the Rate of Global Warming. *Science* **2010**, *327*, 1219–1223. [CrossRef] [PubMed]
2. Vogel, B.; Feck, T.; Grooss, J.U. Impact of stratospheric water vapor enhancements caused by CH_4 and H_2O increase on polar ozone loss. *J. Geophys. Res. Atmos.* **2011**, *116*, 11. [CrossRef]

3. Robrecht, S.; Vogel, B.; Grooß, J.-U.; Rosenlof, K.; Thornberry, T.; Rollins, A.; Krämer, M.; Christensen, L.; Müller, R. Mechanism of ozone loss under enhanced water vapour conditions in the mid-latitude lower stratosphere in summer. *Atmos. Chem. Phys.* **2019**, *19*, 5805–5833. [CrossRef]
4. Shindell, D.T. Climate and ozone response to increased stratospheric water vapor. *Geophys. Res. Lett.* **2001**, *28*, 1551–1554. [CrossRef]
5. Jensen, E.J.; Pan, L.L.; Honomichl, S.; Diskin, G.S.; Krämer, M.; Spelten, N.; Günther, G.; Hurst, D.F.; Fujiwara, M.; Vömel, H.; et al. Assessment of Observational Evidence for Direct Convective Hydration of the Lower Stratosphere. *J. Geophys. Res. Atmos.* **2020**, *125*, e2020JD032793. [CrossRef]
6. Li, D.; Vogel, B.; Müller, R.; Bian, J.; Günther, G.; Ploeger, F.; Li, Q.; Zhang, J.; Bai, Z.; Vömel, H.; et al. Dehydration and low ozone in the tropopause layer over the Asian monsoon caused by tropical cyclones: Lagrangian transport calculations using ERA-Interim and ERA5 reanalysis data. *Atmos. Chem. Phys.* **2020**, *20*, 4133–4152. [CrossRef]
7. Ueyama, R.; Jensen, E.J.; Pfister, L. Convective Influence on the Humidity and Clouds in the Tropical Tropopause Layer During Boreal Summer. *J. Geophys. Res. Atmos.* **2018**, *123*, 7576–7593. [CrossRef]
8. Randel, W.J.; Wu, F.; Russell, J.M.; Roche, A.; Waters, J.W. Seasonal cycles and QBO variations in stratospheric CH_4 and H_2O observed in UARS HALOE data. *J. Atmos. Sci.* **1998**, *55*, 163–185. [CrossRef]
9. Tao, M.; Konopka, P.; Ploeger, F.; Yan, X.; Wright, J.S.; Diallo, M.; Fueglistaler, S.; Riese, M. Multitimescale variations in modeled stratospheric water vapor derived from three modern reanalysis products. *Atmos. Chem. Phys.* **2019**, *19*, 6509–6534. [CrossRef]
10. Tao, M.; Konopka, P.; Ploeger, F.; Riese, M.; Müller, R.; Volk, C.M. Impact of stratospheric major warmings and the quasi-biennial oscillation on the variability of stratospheric water vapor. *Geophys. Res. Lett.* **2015**, *42*, 4599–4607. [CrossRef]
11. Glaze, L.S.; Baloga, S.M.; Wilson, L. Transport of atmospheric water vapor by volcanic eruption columns. *J. Geophys. Res.-Atmos.* **1997**, *102*, 6099–6108. [CrossRef]
12. Murcray, D.G.; Murcray, F.J.; Barker, D.B.; Mastenbrook, H.J. Changes in Stratospheric Water Vapor Associated with the Mount St. Helens Eruption. *Science* **1981**, *211*, 823–824. [CrossRef] [PubMed]
13. Sioris, C.E.; Malo, A.; McLinden, C.A.; D'Amours, R. Direct injection of water vapor into the stratosphere by volcanic eruptions. *Geophys. Res. Lett.* **2016**, *43*, 7694–7700. [CrossRef]
14. Schwartz, M.J.; Read, W.G.; Santee, M.L.; Livesey, N.J.; Froidevaux, L.; Lambert, A.; Manney, G.L. Convectively injected water vapor in the North American summer lowermost stratosphere. *Geophys. Res. Lett.* **2013**, *40*, 2316–2321. [CrossRef]
15. McCormick, M.P.; Thomason, L.W.; Trepte, C.R. Atmospheric effects of the Mt Pinatubo eruption. *Nature* **1995**, *373*, 399–404. [CrossRef]
16. Pitari, G.; Mancini, E. Short-term climatic impact of the 1991 volcanic eruption of Mt. Pinatubo and effects on atmospheric tracers. *Nat. Hazards Earth Syst. Sci.* **2002**, *2*, 91–108. [CrossRef]
17. Bates, S.; Carlowicz, M. Tonga Volcano Plume Reached the Mesosphere. Available online: https://earthobservatory.nasa.gov/images/149474/tonga-volcano-plume-reached-the-mesosphere (accessed on 21 April 2022).
18. Kubota, T.; Saito, T.; Nishida, K. Global fast-traveling tsunamis driven by atmospheric Lamb waves on the 2022 Tonga eruption. *Science* **2022**. [CrossRef] [PubMed]
19. Matoza, R.S.; Fee, D.; Assink, J.D.; Iezzi, A.M.; Green, D.N.; Kim, K.; Toney, L.; Lecocq, T.; Krishnamoorthy, S.; Lalande, J.-M.; et al. Atmospheric waves and global seismoacoustic observations of the January 2022 Hunga eruption, Tonga. *Science* **2022**. [CrossRef]
20. Yuen, D.A.; Scruggs, M.A.; Spera, F.J.; Zheng, Y.; Hu, H.; McNutt, S.R.; Thompson, G.; Mandli, K.; Keller, B.R.; Wei, S.S.; et al. Under the surface: Pressure-induced planetary-scale waves, volcanic lightning, and gaseous clouds caused by the submarine eruption of Hunga Tonga-Hunga Ha'apai volcano. *Earthq. Res. Adv.* **2022**, 100134. [CrossRef]
21. Livesey, N.J.; Read, W.G.; Wagner, P.A.; Froidevaux, L.; Lambert, A.; Manney, G.L.; Valle, L.F.M.; Pumphrey, H.C.; Santee, M.L.; Schwartz, M.J.; et al. *Earth Observing System (EOS), Aura Microwave Limb Sounder (MLS), Version 4.2 x Level 2 and Level 3 Data Quality and Description Document, Version 4.2 x-4.0, D-33509*; Technical Report; Jet Propulsion Laboratory: Pasadena, CA, USA, 2020. Available online: http://mls.jpl.nasa.gov/ (accessed on 20 April 2022).
22. Vömel, H.; Barnes, J.E.; Forno, R.N.; Fujiwara, M.; Hasebe, F.; Iwasaki, S.; Kivi, R.; Komala, N.; Kyrö, E.; Leblanc, T.; et al. Validation of Aura Microwave Limb Sounder water vapor by balloon-borne Cryogenic Frost point Hygrometer measurements. *J. Geophys. Res.* **2007**, *112*, D24S37. [CrossRef]
23. Bian, J.; Pan, L.L.; Paulik, L.; Vömel, H.; Chen, H.; Lu, D. In situ water vapor and ozone measurements in Lhasa and Kunming during the Asian summer monsoon. *Geophys. Res. Lett.* **2012**, *39*, L19808. [CrossRef]
24. Li, D.; Vogel, B.; Bian, J.; Müller, R.; Pan, L.L.; Günther, G.; Bai, Z.; Li, Q.; Zhang, J.; Fan, Q.; et al. Impact of typhoons on the composition of the upper troposphere within the Asian summer monsoon anticyclone: The SWOP campaign in Lhasa 2013. *Atmos. Chem. Phys.* **2017**, *17*, 4657–4672. [CrossRef]
25. Ma, D.; Bian, J.; Li, D.; Bai, Z.; Li, Q.; Zhang, J.; Wang, H.; Zheng, X.; Hurst, D.F.; Vömel, H. Mixing characteristics within the tropopause transition layer over the Asian summer monsoon region based on ozone and water vapor sounding data. *Atmos. Res.* **2022**, *271*, 106093. [CrossRef]
26. Vömel, H.; Tatjana, N.; Ruud, D.; Michael, S. An update on the uncertainties of water vapor measurements using cryogenic frost point hygrometers. *Atmos. Meas. Tech.* **2016**, *9*, 3755–3768. [CrossRef]
27. Hersbach, H.; Bell, B.; Berrisford, P.; Hirahara, S.; Horanyi, A.; Munoz-Sabater, J.; Nicolas, J.; Peubey, C.; Radu, R.; Schepers, D.; et al. The ERA5 global reanalysis. *Q. J. R. Meteorol. Soc.* **2020**, *146*, 1999–2049. [CrossRef]

28. Yan, X.L.; Wright, J.S.; Zheng, X.D.; Livesey, N.J.; Vomel, H.; Zhou, X.J. Validation of Aura MLS retrievals of temperature, water vapour and ozone in the upper troposphere and lower-middle stratosphere over the Tibetan Plateau during boreal summer. *Atmos. Meas. Tech.* **2016**, *9*, 3547–3566. [CrossRef]
29. Danielsen, E.F. Trajectories of the Mount St. Helens Eruption Plume. *Science* **1981**, *211*, 819–821. [CrossRef] [PubMed]
30. Carey, S.; Sigurdsson, H.; Gardner, J.E.; Criswell, W. Variations in column height and magma discharge during the May 18, 1980 eruption of Mount St. Helens. *J. Volcanol. Geotherm. Res.* **1990**, *43*, 99–112. [CrossRef]
31. Rutherford, M.J.; Sigurdsson, H.; Carey, S.; Davis, A. The May 18, 1980, eruption of Mount St. Helens: 1. Melt composition and experimental phase equilibria. *J. Geophys. Res.* **1985**, *90*, 2929–2947. [CrossRef]
32. Butchart, N. The Brewer–Dobson circulation. *Rev. Geophys.* **2014**, *52*, 157–184. [CrossRef]
33. Plumb, R.A. Stratospheric transport. *J. Meteorol. Soc. Jpn.* **2002**, *80*, 793–809. [CrossRef]
34. Tegtmeier, S.; Rex, M.; Wohltmann, I.; Krüger, K. Relative importance of dynamical and chemical contributions to Arctic wintertime ozone. *Geophys. Res. Lett.* **2008**, *35*, L17801. [CrossRef]
35. Lubis, S.W.; Silverman, V.; Matthes, K.; Harnik, N.; Omrani, N.-E.; Wahl, S. How does downward planetary wave coupling affect polar stratospheric ozone in the Arctic winter stratosphere? *Atmos. Chem. Phys.* **2017**, *17*, 2437–2458. [CrossRef]
36. Zhang, H.; Wang, F.; Li, J.; Duan, Y.; Zhu, C.; He, J. Potential Impact of Tonga Volcano Eruption on Global Mean Surface Air Temperature. *J. Meteorol. Res.* **2022**, *36*, 1–5. [CrossRef]
37. Zuo, M.; Zhou, T.; Man, W.; Chen, X.; Liu, J.; Liu, F.; Gao, C. Volcanoes and Climate: Sizing up the Impact of the Recent Hunga Tonga-Hunga Ha'apai Volcanic Eruption from a Historical Perspective. *Adv. Atmos. Sci.* **2022**. [CrossRef]